Chaouch Abdellah [1], Meflah Abderrahmane M.R[1] , Kheiter Amel[1], Chouitek mama[2]

Department of Electrical Engineering, Mostaganem University, Laboratory of Renewable Energies and Electrical Systems Mostaganem, Algeria (1), Maintenance and Industrial Safety Institute, University Es Senia 2 of Oran, Oran 31000, Algeria (2)

doi:10.15199/48.2023.08.39:

Park's Vector Approach to Detect Broken Rotor Bars in Saturated Induction Motor

Abstract. *This paper deals with the problem of broken rotor bars fault diagnosis in saturated induction motor. Several techniques such as those based on vibration, axial leakage monitoring, zero-sequence component, negative sequence current, and motor current signature analysis have been used. However, these techniques do not take into account the effect of magnetic saturation. This paper presents a current Park's Vector method for diagnosis in squirrel cage induction motor with the presence of magnetic saturation. The use of a current vector pattern trajectory and Modulus current spectrum analysis demonstrate that deformation of the Current Park's Vector Pattern trajectory and the presence of new harmonics are indicators for predicting magnetic saturation and broken bars rotor fault. Our experimental results allow us to discriminate between the magnetic saturation in healthy and faulty squirrel cage induction motors.*

Streszczenie. *W artykule podjęto problematykę diagnostyki pękniętych prętów wirnika w nasyconym silniku indukcyjnym. Zastosowano kilka technik, takich jak oparte na drganiach, monitorowaniu upływu osiowego, składowej zerowej, składowej przeciwnej prądu i analizie sygnatur prądu silnika. Techniki te nie uwzględniają jednak wpływu nasycenia magnetycznego. W artykule przedstawiono aktualną metodę Parka Vector do diagnostyki silnika indukcyjnego klatkowego z obecnością nasycenia magnetycznego. Wykorzystanie trajektorii wektora prądu i analiza widma prądu modułowego pokazują, że deformacja trajektorii wzorca wektorowego Current Park i obecność nowych harmonicznych są wskaźnikami do przewidywania nasycenia magnetycznego i uszkodzenia wirnika z pękniętymi prętami. Nasze wyniki eksperymentalne pozwalają nam rozróżnić nasycenie magnetyczne w zdrowych i uszkodzonych silnikach indukcyjnych klatkowych. (**Metoda wektorowa Parka do wykrywania pękniętych prętów wirnika w nasyconym silniku indukcyjnym**)*

Keywords: Broken bar, Modulus Current Park, Diagnosis, Induction motor, Magnetic saturation.
Słowa kluczowe: uszkodzony pręt, Modulus Current Park, Diagnoza, Silnik indukcyjny, Nasycenie magnetyczne.

.

Introduction

In industrial applications, squirrel cage induction motors (SCIMs) are popularly used due to their robustness, reliability, and low cost. However, during their operation, induction machines are frequently subjected to a variety of stresses (e.g., excessive heating or the rotor is subjected to electromagnetic forces and environmental stresses during normal use, resulting in magnetic fatigue). These stresses generate problems in various components of the machine such as broken bar rotor faults; rotor fault occurs from thermal stresses: hot spot or fatigue stress that occurs during transient operation such as when starting up a large motor [1–8].

A broken bar rotor is very difficult to detect because a SCIM with this fault continues working without giving any indication of the failure. For these reasons, several authors are interested in diagnostic methods for a broken bar [9–12]. To detect machine faults using physical parameters, various fault detection methods have been established, such as current, voltage, speed, efficiency, temperature, and vibration. Many techniques for monitoring the health of and detecting faults in SCIMs are based on the processing of stator line currents [13–17]. Among these, different authors have used Park's Vector technique to analyze various types of individual faults [18–26].

Several published works are related to rotor bar failures in squirrel cage induction motors are based on machine current signature analysis. In this way fast Fourier transform is used to show the effect of this fault on frequency spectrum of current signal. Broken rotor bars in squirrel cage induction machine results the presence of two sidebands frequency in the stator current spectrum.

However, in much of the research concerning fault diagnosis, the magnetic saturation is not considered in the model. Recently, many researchers have tended to move towards the introduction of the phenomenon of saturation in their motor's modeling to give more details concerning the diagnosis of faults and on optimal design.

In [27], magnetic saturation is introduced by the Finite Element Method (FEM), which demonstrates the saturation effect when an induction motor is under voltage fluctuations. In [28], an approach based on a zero sequence current component (ZSC) is proposed for fault diagnosis including the effects of magnetic core saturation. In [29], an approach based on winding function and the saturation core effect are utilized for broken bar rotor detection. In [30], we have shown via spectral analysis of the stator current that, on the one hand, the saturation harmonic was close to characterizing the properties of the asynchronous motor and, on the other hand, in the faulty motor.

From the above survey, we can observe that there is a continuing tread to develop a method for broken rotor bar fault diagnosis, and different modeling for magnetic saturation. However, this phenomena is not considered in fault diagnosis. This leads to our objective of this paper, that is, to achieve broken rotor bar fault diagnosis with take in consideration the magnetic saturation.

The aim of this paper is to use the Current Park's Vector Approach (CPVA) and the Modulus of the Current Park (MCPA) to show the effect of magnetic saturation and its difficulty in discriminating between the healthy, faulty, and saturate motor.

The modeling of saturated SCIM

We study an Induction Motor (IM) having n rotor bars and m stator circuits. Voltage equations for the SCIM are written as follows:

$$[V_s] = [R_s][I_s] + \frac{d[\psi_s]}{dt} \quad (1)$$

$$[V_r] = [R_r][I_r] + \frac{d[\psi_r]}{dt} \quad (2)$$

Voltage and currents for stator and rotor are given by

$$[V_s] = [v_1^s v_2^s \dots v_m^s]^T, \quad [V_r] = [00\dots0]^T \quad (3)$$

(4) $$[I_s]=\left[i_1^s\, i_2^s \dots v_m^s\right]^T, [I_r]=\left[i_1^r\, i_2^r \dots v_n^r\right]^T$$

and flux linkages for stator and rotor are given by

(5) $$[\psi_s]=[L_{ss}][I_s]+[L_{rs}][I_r]$$

(6) $$[\psi_r]=[L_{rr}][I_r]+[L_{rs}][I_s]$$

L_{ss} and L_{rr} are self and mutual inductances for stator and rotor respectively, L_{sr} is the mutual inductances between the rotor loops and the stator phases, with $L_{sr} = L_{rs}^t$.

The dynamic equations for the SCIM are

(7) $$J\frac{d\,\omega_r}{dt}+T_L=T_e$$

(8) $$\frac{d\,\theta_r}{dt}=\omega_r$$

where J is the rotor inertia, ω is mechanical speed and θ_r is the angular position. T_L and T_e is load and electromagnetic torque respectively.

The electromagnetic torque is represented as

(9) $$T_e=\frac{1}{2}\left[I_s^t L_{ss} I_s + I_s^t L_{sr} I_r + I_r^t L_{rs} I_s + I_r^t L_{rr} I_r\right]$$

The mathematical model of magnetic saturation is represented by a variation the air gap in function with position and saturation level, this function is written as [1]:

(10) $$g_s(\phi,\theta)\approx g'\left[1-k_{gsat}\cos\{2(p\phi-\theta)\}\right]$$

(11) $$g_s^{-1}(\phi,\theta)\approx\frac{1}{g'}\left[1+k_{gsat}\cos\{2(p\phi-\theta)\}\right]$$

Where, k_{gsat} is the saturation factor, g' is average value of the air-gap, θ is the position of the air-gap flux, p is the number of pole pairs, ϕ and is the stator position.

The variation of the air gap length means changing in different inductances and therefore the performance of the inductor motor. We have demonstrated this variation in our Work [31].

Modeling by CPVA and MCPA

The method is based on the transformation of a three-phase system to two and simplifies its study, for this reason CPVA [16] is widely used in electrical control and in the study of transient regimes of electrical networks.

(12) $$i_d=\left(\frac{\sqrt{2}}{\sqrt{3}}\right)i_a-\left(\frac{1}{\sqrt{6}}\right)i_b-\left(\frac{1}{\sqrt{6}}\right)i_c$$

(13) $$i_q=\left(\frac{1}{\sqrt{2}}\right)i_b-\left(\frac{1}{\sqrt{2}}\right)i_c$$

with mathematical transformation, we can write:

(14) $$i_d=\left(\frac{\sqrt{2}}{6}\right)i_M\sin(\omega t)$$

(15) $$i_q=\left(\frac{\sqrt{2}}{6}\right)i_M\sin\left(\omega t-\frac{\pi}{2}\right)$$

(16) $$I=\sqrt{i_d^2+i_q^2}$$

Where I represent Park Vector Modulus (PVM).

CPVA is represented by a circle. This geometric shape represents the ideal operation of the machine (fig. 1). This locus is distorted by saturation, broken faults and thus provides easy fault diagnosis. PVM as a function of time represents distortion in the fault diagnosis signal or the presence of harmonics in its spectrum frequency analysis.

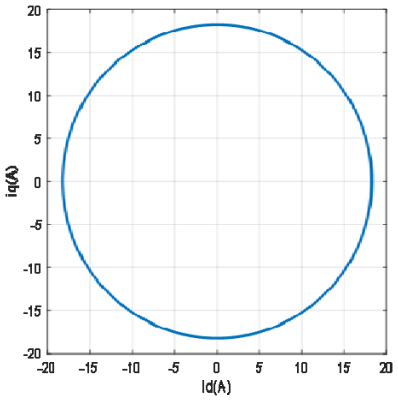

Fig. 1. Park's Vector Pattern for a healthy motor and an ideal case.

Experimental results

Test bench details

In order to use CPVA in our experimental study, we have mounted a test bench is depicted in fig. 2. The test bench is made up of an asynchronous motor (SCIM), the specifications of the induction motors are shown in Table I. The motor drives a permanent magnet synchronous generator (GSAPM) supplying a variable resistive load. For the fault diagnostic test we replace the healthy motor by a faulty in our case a broken bar rotor. Fig. 3 and fig. 4 show the different elements of the test bench and pictures of healthy and broken bar rotor respectively.

Table 2. Squirrel Cage Induction Motor Specifications.

Specifications	Unit	Value
Power	kW	8
Voltage	Volt	380
Rated current	Amp	9
Speed	RPM	1425
Frequency	Hz	50
Rotor bars	-	28

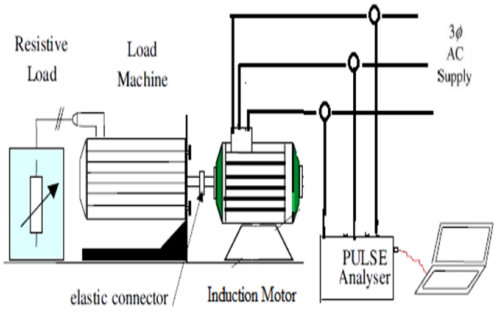

Fig. 2. Detection system scheme.

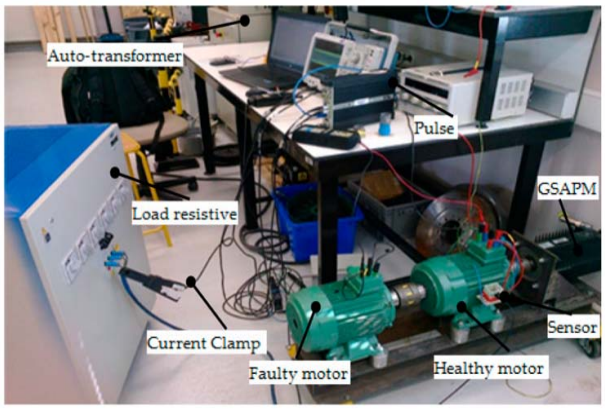

Fig. 3. Experimental bench test.

Fig. 4. Pictures of a healthy and a broken bar rotor.

Results and Discussion*:*

To show the effect of saturation in our study, we have tested motor at no load, we noted that the voltage-current characteristic (Fig. 5), and we deduced the saturation factor in which the voltage applied to reach the saturation of the machine.

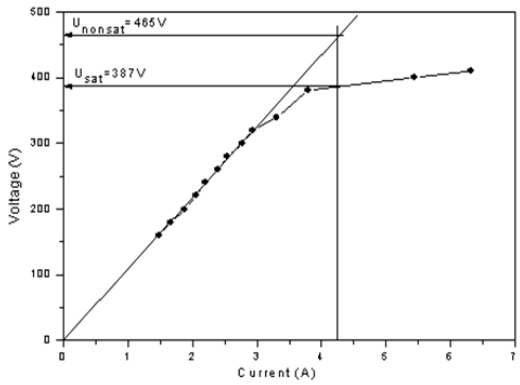

Fig. 5. No-load characteristic of the experimental motor.

CPVA Trajectories

Fig. 6 and fig. 7 present the Current Parks Vector Pattern trajectories for the healthy motor with and without load for both cases with and without saturation.

The trajectories have a different shape of the circle because of the non-sinusoid of the power source. The saturation effect is marked by the increase of the diameter of the hexagonal shape at no loaded motor (fig. 6), in the loaded and without saturation case the current path rotates 90 ° and when the motor is saturated in addition of increasing the diameter, we notice the deformation of the hexagonal shape (fig. 7).

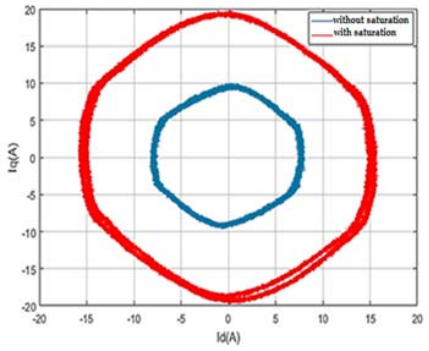

Fig. 6. Experimental CPVP for healthy motor at no load.

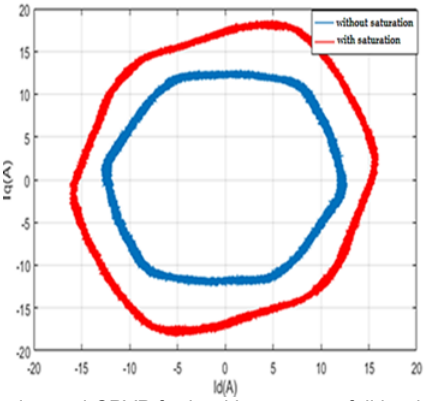

Fig. 7. Experimental CPVP for healthy motor at full load.

Fig 8 shows the current park pattern without saturation for healthy (blue) and broken bar rotor fault (red). It could be seen that broken bar fault is detected by the increase of the thickness of the shape. Fig 9 shows the current park pattern with saturation likewise for healthy and broken bar rotor fault. In this case with saturation, it could be seen that the magnetic saturation cause a clear deformation of the park current trajectories with the thick of shape for broken bar rotor.

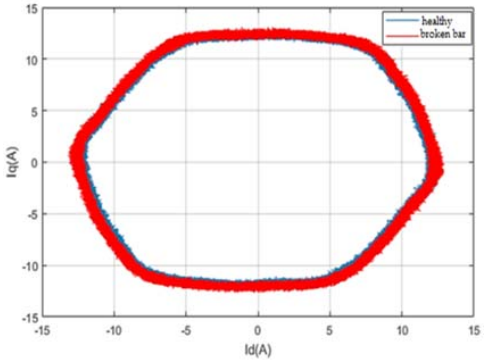

Fig. 8. Motor without saturation.

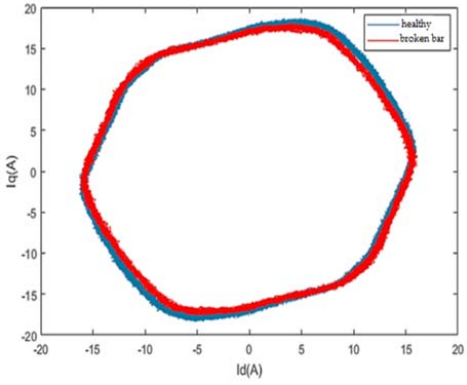

Fig. 9 Motor with saturation

Using the Current Parks Vector Pattern, the visual examination of the shape thickness by a non-expert person can be considered as the first reliable broken fault existence indicator, and the increase of Diameter with deformation of the shape are magnetic saturation indicator. Unlike the majority of techniques, Current Parks Vector Pattern can provide accurate information about rotor health without requiring access to the motor.

Spectrum Analysis of PVM

Fig. 10 and fig. 11 present the spectrum frequency analysis of PVM for the healthy motor with load for both cases with and without saturation. Figures (10 and 11) show the presence of the principal harmonics components (PH_1, PH_2 and PH_3). Figure 11 is marked by the presence of saturation harmonic component identified at approximately 1.2 Hz.

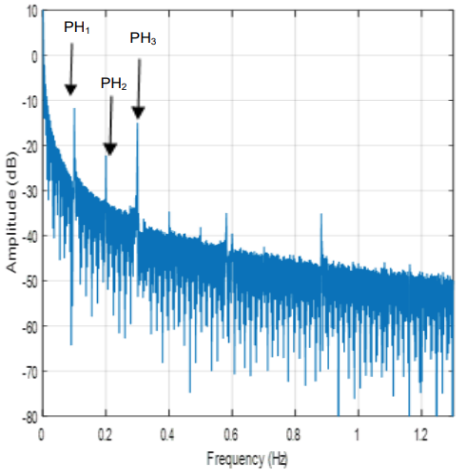

Fig. 10 Spectrum analysis of PVM for healthy Motor and without saturation.

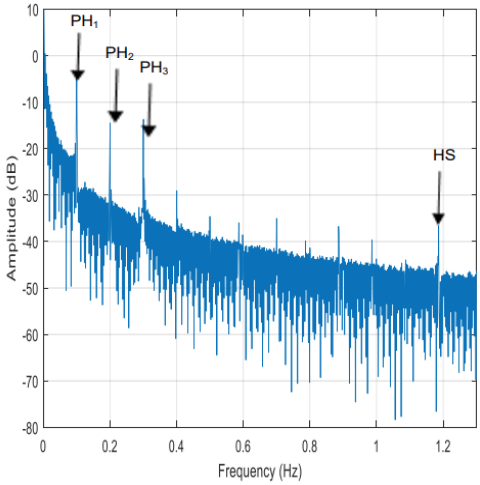

Fig.11 Spectrum analysis of PVM for healthy Motor and with saturation.

Figure 12 shows the PVM spectrum for faulty motor without saturation. The Broken harmonic (BH) is detected in the neighbourhood of the principal harmonics.
For the case of the faulty motor with saturation (Figure 13), the broken harmonics are in the proximity of the saturation harmonic position. In this experimental stydies, we can see the absence of broken bar harmonic BH1 (fig.13) when the motor is saturated. This demonstrate that the difficult to discriminate between saturation and faulty motor.

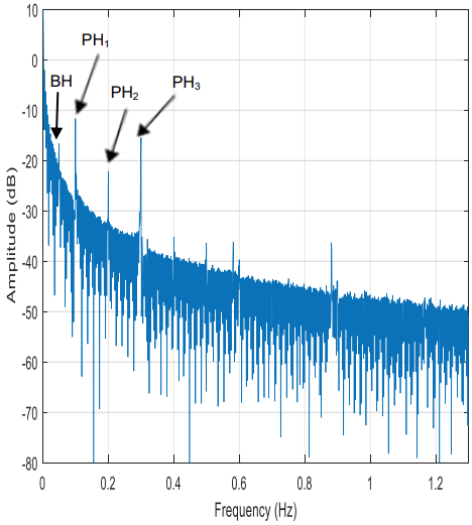

Fig. 12 Spectrum analysis of PVM for broken bar rotor and without saturation

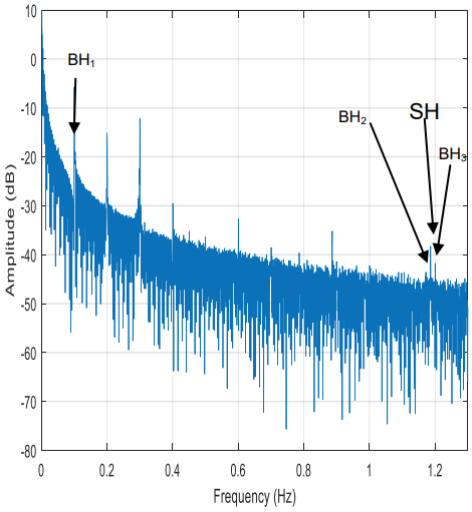

Fig. 13 Spectrum analysis of PVM for broken bar rotor and saturation.

Conclusion

This paper presents the magnetic saturation effect on fault diagnosis in SCIM using Current Parks Vector Pattern (CPVP) technique and spectrum analysis of PVM.

In the CPVP For healthy motor without saturation, the trajectory was hexagonal shape while with saturation the diameter of the CPVP shape rise. The increasing of the thickness CPVP trajectory of broken bar is indexes diagnosis for SCIM without and with saturation.

In the spectrum analysis of PVM shows clearly the presence of saturation harmonic in health and faulty motor.

The analysis of the Park's vector patterns allows for obtaining a simple graphical view of the presence of abnormal operating conditions. This is an efficient method to detect an incipient rotor bar fault easily and early on without the need of the user expertise to interpret the obtained diagnosis results. However, the pattern does not give an accurate quantitative idea as to the magnitude of the problem.

The magnetic saturation is manifested by the increase in the diameter of the PCVP shape and by its deformation of the trajectory. The increase in shape diameter is an effective indicator for healthy motor operation in the region of saturation. Nevertheless, the deformation and the change of the shape CPVP in the case where the motor presents a

broken rotor bar, it is difficult to decide that they are indicators of the presence of saturation, because the deformation and the change of the shape CPVP may be signs of short winding or bearing faults as demonstrated in reference [23-24] and [27]. In the other hand the presence of saturation harmonic is clearly detected by spectrum analysis of PVM.

In the next paper, we validate the effectiveness of PCVP and PVM technique when we are the combined faults like eccentricity and bearing faults with and without magnetic saturation.

REFERENCES

[1] Seong, H, I and Bon,G,G. Study of Induction Motor Inter-Turn Fault Part II: Online Model Based Fault Diagnosis Method, Energies 2022, 15, 977. DOI: 10.3390/en15030977

[2] Ahmed, R. Faults diagnosis in stator windings of high speed solid rotor induction motors using fuzzy neural network, International Journal of Power Electronics and Drive Systems, 2021, 12(1), pp.597-611. DOI:10.11591/ijpeds.v12.i1.pp597-611.

[3] Biswarup, G, Arpan, C, Arunava, C and all, Diagnosis of Stator Winding Fault of Single-Phase Induction Motor Employing Wavelet Induced Residual-Convolutional Neural Network, IEEE International conference on power electronics, Drives and Energy System (PEDES), 16-19 Dec 2020, DOI: 10.1109/PEDES49360.2020.9379665

[4] Mohammed, S, J, B, Jassim, M, H. Inter-Turn Stator Winding Faults Diagnosis in Three-Phase Induction Motor Fed from Imbalanced Voltage Source, Journal of Engineering and Applied Sciences, 2019, pp.7591-7598. DOI: 10.36478/jeasci.2019.7591.7598.

[5] Reljic, D, Jerkan, D. Broken Bar Fault Detection in IM Operating Under No-Load Condition, Advances in Electrical and Computer Engineering 16(4):63-70, 2016. DOI: 10.4316/AECE.2016.04010

[6] Zolfaghari, S.; Noor, S.B.M.; Mehrjou, M.R.; Marhaban, M.H.; Mariun, N. Broken Rotor Bar Fault Detectionand Classification Using Wavelet Packet Signature Analysis Based on Fourier Transform and Multi-Layer Perceptron Neural Network. Appl. Sci. 2017, 8, 25.

[7] Edomwandekhoe, K and Liang, X, Advanced feature selection for broken rotor bar faults in induction motors, Proceedings of 2018 IEEE/IAS 54th Industrial and Commercial Power Systems Technical Conference (I&CPS), pp. 1-10, May 2018.

[8] Wang, Z, Yang, J, Li, H, Zhen , D, Xu, Y and Gu, F, Fault Identification of Broken Rotor Bars in Induction Motors Using an Improved Cyclic Modulation Spectral Analysis, Energies, vol. 12, no. 17, p. 3279, Jan. 2019.

[9] Nemec, M.; Ambroži˘c, V.; Fišer, R.; Nedeljkovi´c, D.; Drobni˘c, K. Induction Motor Broken Rotor Bar Detection Based on Rotor Flux Angle Monitoring. Energies 2019, 12, 794.

[10] Dias, C.G.; da Silva, L.C.; Luz Alves, W.A. A Histogram of Oriented Gradients Approach for Detecting Broken Bars in Squirrel-Cage Induction Motors. IEEE Trans. Instrum. Meas. 2020, 69, 6968–6981.

[11] Fernandez-Cavero, V.; Pons-Llinares, J.; Duque-Perez, O.; Morinigo-SOTELO, D. Detection of Broken Rotor Bars in Non-Linear Startups of Inverter-Fed Induction Motors. IEEE Trans. Ind. Appl. 2021, 57, 2559–2568.

[12] Li, H., Feng, G., Zhen, D., Gu, F., & Ball, A. D. (2021). A Normalized Frequency-Domai Energy Operator for Broken Rotor Bar Fault Diagnosis. IEEE Transactions on Instrumentation and Measurement, 70. DOI: 10.1109/TIM.2020.3009011

[13] Noman, S, Lauri, K, Bilal, A, Muhammad, J, and all, Spectrum Analysis for Condition Monitoring and Fault Diagnosis of Ventilation Motor: A Case Study, Energies 2021, 14, 2001. DOI: 10.3390/en14072001

[14] Park, Y, S. Investigation on Electromagnetic Performance of Induction Motor with Rotor Bar Faults considering Motor Current Signals, Advances in Electrical and Computer Engineering 20(4), pp.37-40, 2020. DOI: 10.4316/AECE.2020.04005

[15] Ojeda-Aguirre, N, A, Garcia-Perez, A, and all. Reassigned Short Time Fourier Transform and K-means Method for Diagnosis of Broken Rotor Bar Detection in VSD-fed Induction Motors, Advances in Electrical and Computer Engineering 19, pp.61-68, 2019. DOI: 10.4316/AECE.2019.02008.

[16] Bessous, N., Sbaa, S. & Megherbi, A. C. Mechanical fault detection in rotating electrical machines using MCSA-FFT and MCSA-DWT techniques. Bulletin of the Polish Academy of Sciences: Technical Sciences, Vol 67(3), 571-582. DOI: 10.24425/bpasts.2019.129655

[17] Matic, D, Kanovic, Z. Vibration Based Broken Bar Detection in Induction Machine for Low Load Conditions, Advances in Electrical and Computer Engineering, 17 pp.63-70, 2017. DOI: 10.4316/AECE.2017.01007.

[18] Mustapha, M , Aymen, F , Abdullah A, A, and all, Diagnosis and Fault Detection of Rotor Bars in Squirrel Cage Induction Motors Using Combined Park's Vector and Extended Park's Vector Approaches, Electronics 2022, 11, 380. DOI: 10.3390/electronics11030380

[19] Shurong, W; Xin, Z ; Yao, X ; Yang, F ,Zixu ,R ; Fangxing, L, Extended Park's vector method in early inter-turn short circuit fault detection for the stator windings of offshore wind doubly-fed induction generators, IET Generation, Transmission & Distribution, Vol 14, Issue 18, 18 September 2020, p. 3905 – 3912, DOI: 10.1049/iet-gtd.2020.0127.

[20] Fatima, H; Jeevan, S, and All, Inter-Turn Fault Diagnosis of Induction Motor Fed by PCC-VSI Using Park Vector Approach, 2020 IEEE International Conference on Power Electronics, Drives and Energy Systems (PEDES) , 16-19 Dec. 2020, DOI: 10.1109/PEDES49360.2020.9379388.

[21] Gyftakis, K.N., Cardoso, A.J.M., Daviu, J.A.A. Introducing the Filtered Park's and Filtered Extended Park's Vector Approach to detect broken rotor bars in IM. Mech. Syst. Signal Proc. 2017, 93, 30–50.

[22] Tushar, G, V, Makarand, B, S, and Hiralal, S, M, Application of Multiple Parks Vector Approach for Detection of Multiple Faults in Induction Motors, Journal of Power Electronics, Vol. 17, No. 4, pp. 97982, July 2017. DOI: 10.6113/JPE.2017.17.4.972

[23] Izzet Yilmaz, O, N, Mohamed, B. Induction motor bearing failure detection and diagnosis: Park and Concordia Transform Approaches Comparative study, IEEE/ASME Trans. Mechatronics, Vol.13, No.2,pp.257-262, April 2008.

[24] Marques Cardoso, A.J. Inter-turn stator winding fault diagnosis in three-phase induction motors, by Park's vector approach, IEEE Trans. Energy Conversion, Volume: 14, pp. 595 - 598, Sep 1999.

[25] Nejjari, H, Benbouzid, M.H. Monitoring and diagnosis of induction motor faults using current parks vector approach, IEEE trans. Ind.Applicat.,,vol.36,no.3,May/June 2000, pp.730 – 735.

[26] Cruz, S, M, A. Stator winding fault diagnosis in three-phase synchronous and asynchronous motors, by the extended Park's vector approach, IEEE conf. Ind. Applicat., vol.1, pp. 395 – 401, 2000

[27] Jasmin, P, Saranya, R, Indragandhi, V, and all, 2D Finite Element Analysis of Asynchronous Machine Influenced Under Power Quality Perturbations, Computers, Materials & Continua 2022, vol.70, no.3, DOI:10.32604/cmc.2022.020093.

[28] Arkadiusz, D, and Piotr, D, Induction Motor Fault Diagnosis Based on Zero-Sequence Current Analysis, Energies 2020, 13, 6528, DOI: 10.3390/en13246528.

[29] Mehrdad, G, Om-Kolsoom, S, Hadi, T, An extended winding function model for induction machine modelling considering saturation effect, IET Electr. Power Appl. 2021, 15, 79–91, DOI:10.1049/elp2.12006.

[30] Chaouch, A. Bendiabdellah, P. Remus, R.Romary , J.P. Lecointe, "Mixed Eccentricity Fault Diagnosis in Saturated Squirrel Cage Induction Motor using Instantaneous Power Spectrum Analysis" ,PRZEGLĄD ELEKTROTECHNICZNY, ISSN 0033-2097, R. 92, NR 7/2016,

[31] Chaouch, A. et A.Bendiabdellah, " Mixed Eccentricity Fault Diagnosis in Saturated Squirrel Cage Induction Motor", International Review on Modelling and Simulations (IREMOS), vol. 5,No.3, June 2012.